1000-0569/2015/031(06)-1621-35 *Acta Petrologica Sinica* 岩石学报

华北克拉通南缘1600Ma麻坪A型花岗岩的成因及其地质意义*

邓小芹[1,2] 赵太平[1**] 彭头平[3] 高昕宇[1] 包志伟[1]

DENG XiaoQin[1,2], ZHAO TaiPing[1**], PENG TouPing[3], GAO XinYu[1] and BAO ZhiWei[1]

1. 中国科学院广州地球化学研究所矿物学与成矿学重点实验室,广州 510640
2. 中国科学院大学,北京 100049
3. 中国科学院广州地球化学研究所同位素地球化学国家重点实验室,广州 510640

1. *Key Laboratory of Mineralogy and Metallogeny, Guangzhou Institute of Geochemistry, Chinese Academy of Sciences, Guangzhou* 510640, *China*
2. *University of Chinese Academy of Sciences, Beijing* 100049, *China*
3. *State Key Laboratory of Isotope Geochemistry, Guangzhou Institute of Geochemistry, Chinese Academy of Sciences, Guangzhou* 510640, *China*

2014-09-20 收稿, 2014-11-30 改回.

Deng XQ, Zhao TP, Peng TP, Gao XY and Bao ZW. 2015. Petrogenesis of 1600Ma Maping A-type granite in the southern margin of the North China Craton and its tectonic implications. *Acta Petrologica Sinica*, 31(6):1621 – 1635

Abstract The Maping pluton in the southern margin of the North China Craton (NCC) mainly consists of porphyritic granite. Phenocryst minerals include K-feldspar and quartz. LA-ICP-MS zircon U-Pb dating shows that the pluton was emplaced at 1600Ma. All rocks are rich in SiO_2 (70.51% ~ 75.69%) and alkaline ($K_2O + Na_2O$ = 7.42% ~ 10.27%, $K_2O/Na_2O > 23$), but poor in MgO (0.24% ~ 0.58%), CaO (0.06% ~ 0.12%), P_2O_5 (0.04% ~ 0.08%) and MnO (0.01%) with negative Eu, Sr and Ti anomalies, indicating that they experienced fractional crystallization during magmatic evolution. Their high aluminum saturation index (A/CNK > 1.11) show an affinity to that of strongly peraluminous granite. However, their high Ga/Al ratios along with high zircon saturation temperatures (870 ~ 953℃), indicate that the Maping granite porphyry is similar to A-type granite. Combined with their strong peraluminous nature, the Maping granite can be classified as strongly peraluminous A-type granite. Their geochemical signatures, along with zircon Hf isotopic compositions and two-stage model ages of the Maping granite porphyry, suggest that they were dominantly derived from high-temperature partial melting of Taihua Group with the underplating of mafic magmas, which provided heat that triggered partial melting of crust. Integrated with regional data, the generation of the Maping granite porphyry was most likely the products of rifting magmatism that was related to the break-up of the Columbia supercontinent.

Key words A-type granite; Petrogenesis; Mesoproterozoic; Southern margin of the North China Craton; Columbia supercontinent

摘 要 麻坪花岗岩体产于华北克拉通南缘,岩石类型主要为花岗斑岩,具斑状结构,斑晶主要为钾长石和石英。LA-ICP-MS 锆石 U-Pb 定年结果表明,岩体的形成时代为 1600Ma。所有样品高 SiO_2(70.51% ~75.69%)、富碱($K_2O + Na_2O$ = 7.42% ~10.27%,$K_2O/Na_2O > 23$),贫 MgO(0.24% ~0.58%)、CaO(0.06% ~0.12%)、P_2O_5(0.04% ~0.08%)和 MnO(0.01%),以及 Eu、Sr 和 Ti 负异常,表明它们在演化过程中经历了钾长石、斜长石、铁钛氧化物等的分离结晶作用。它们高的铝饱和指数(A/CNK > 1.11),显示强过铝质特征。然而,麻坪花岗斑岩高的 Ga/Al 比值以及高的锆石饱和温度(870 ~953℃),显示典型的 A 型花岗岩特征。因此,麻坪花岗斑岩为强过铝质 A 型花岗岩。麻坪花岗斑岩的地球化学特征、锆石 Hf 同位素组成以及二阶段模式年龄表明其来自太华群高温条件下部分熔融,同时基性岩浆的底侵作用为之提供了相应的热源。麻坪花岗斑岩的产生是裂谷岩浆活动的产物,其形成可能与 Columbia 超大陆的裂解有关。

关键词 A 型花岗岩;成因;中元古代;华北克拉通南缘;Columbia 超大陆

中图法分类号 P588.121; P597.3

---

* 本文受国家重点基础研究发展计划 973 项目(2012CB416606)资助.

第一作者简介:邓小芹,女,1988 年生,博士生,矿物、岩石、矿床学专业,E-mail:deng_xiaoqin@126.com

** **通讯作者**:赵太平,男,1963 年生,研究员,博士生导师,矿物、岩石、矿床学专业,E-mail:tpzhao@gig.ac.cn

1 引言

A 型花岗岩最初由 Loiselle and Wones(1979)提出,代表非造山、碱性和无水的花岗岩,此后其定义范围有所扩大(Collins *et al.*, 1982; Pearce *et al.*, 1984; Whalen *et al.*, 1987; Bonin, 2007)。目前普遍认为,该类花岗岩具有富碱,高 Fe/(Fe + Mg)、Rb/Sr、HFSE,低 Ca、Fe、Mg,强烈亏损 Eu、Sr、Ba、P、Ti 的特点(Collins *et al.*, 1982; King *et al.*, 1997),且常与同时代的基性岩体共生(Haapala and Rämö, 1992)。关于 A 型花岗岩的成因焦点问题在于这类花岗岩是直接来自幔源玄武岩的分异,还是来自单一的地壳部分熔融、抑或是同时有地幔物质的加入(Wu *et al.*, 2002; Yang *et al.*, 2006; Bonin, 2007)。A 型花岗岩的产生通常与伸展的构造背景有关,如造山后或者非造山环境(Frost *et al.*, 2007; Zhao and Zhou, 2009)。因此,A 型花岗岩的研究对于区域地壳的演化和壳幔相互作用以及大地构造演化具有非常重要的指示意义(Collins *et al.*, 1982; Bonin, 2007)。

华北克拉通是世界上最古老的克拉通之一(Zhai *et al.*, 2011),其古元古代活动带的演化结束于 1800Ma 前(翟明国等, 2014),之后在 1800 ~ 1600Ma 发育了一系列的岩浆岩,主要包括不整合覆盖在太古宙和古元古代变质基底上与裂

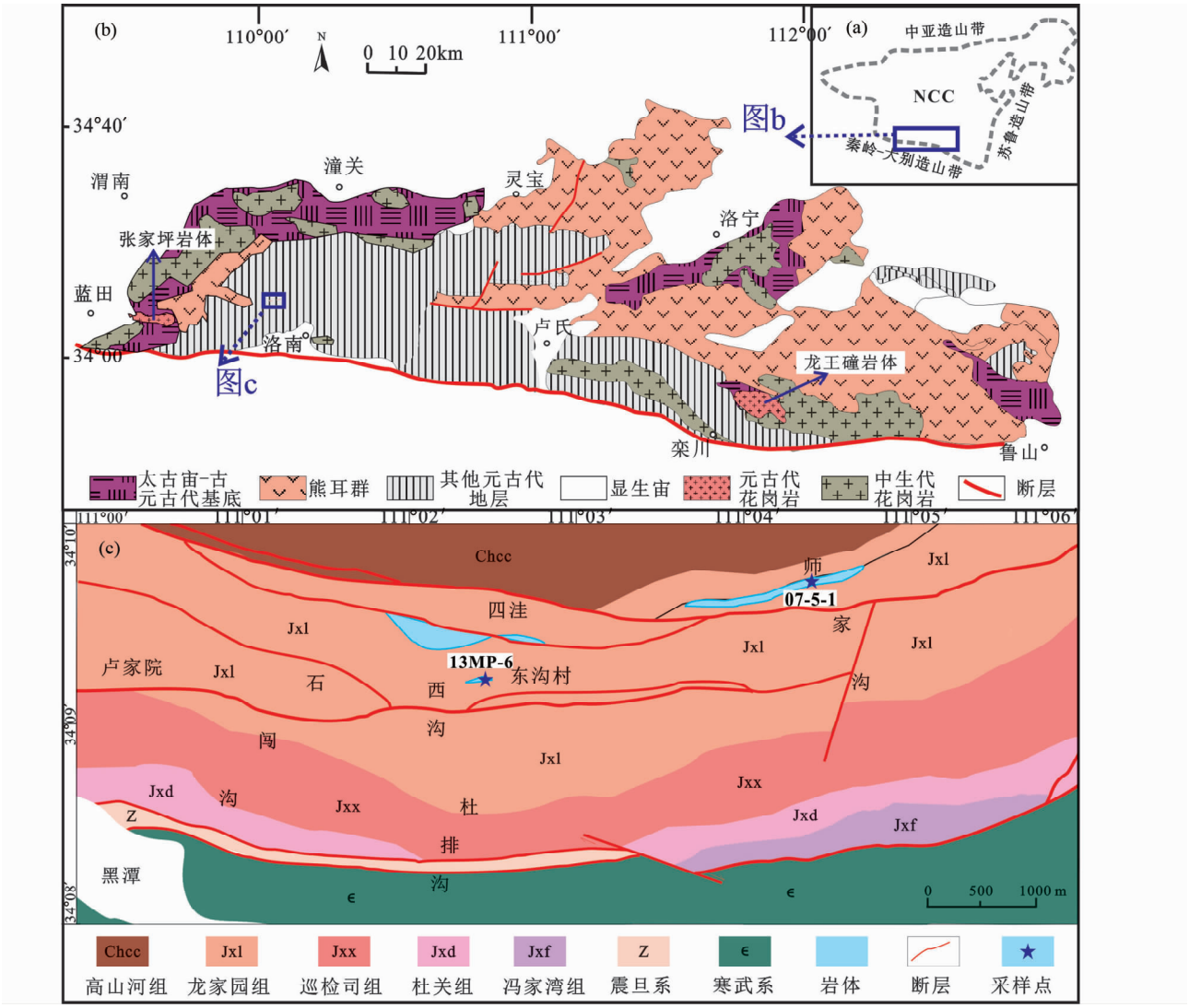

图 1 华北克拉通地质简图(a,据 Peng *et al.*, 2005)、研究区在华北南缘的位置(b 据 Hu *et al.*, 2014)及麻坪地区地质简图(c,据地矿部陕西地勘局,1998①)

Fig. 1 Simplified geological map of the NCC (a, after Peng *et al.*, 2005), the position of the study area in the southern margin of the NCC (b, modified after Hu *et al.*, 2014) and simplified geological map of the Maping area (c)

① 地矿部陕西地勘局. 1998. 1∶5 万洛南县区域地质图和地质报告

谷有关的1.80～1.75Ga熊耳群双峰式火山岩(Zhao *et al.*, 2002；赵太平等, 2004)和1.68～1.62Ga长城系火山-沉积建造(李怀坤等, 1995；Lu *et al.*, 2008),以及与它们同期的基性岩墙群(彭澎等, 2004, 2011；Wang *et al.*, 2004, 2008；胡国辉等, 2010)和1.72～1.60Ga的斜长岩-环斑花岗岩、碱性岩-碱性花岗岩等非造山岩浆活动(杨进辉等, 2005；Zhang *et al.*, 2007, 2013；包志伟等, 2009；Zhao *et al.*, 2009；Zhao and Zhou, 2009；Jiang *et al.*, 2011；Wang *et al.*, 2013)。在这一时期的A型花岗岩也陆续被报道,例如宁夏泾源花岗斑岩(1803±15Ma；高山林等, 2013)、长哨营-古北口正长花岗岩(1753±23Ma和1692±19Ma；Zhang *et al.*, 2007)、密云环斑花岗岩(～1683Ma；Rämö *et al.*, 1995；杨进辉等, 2005；高维等, 2008；李怀坤等, 2011)、温泉花岗岩(～1697Ma；Jiang *et al.*, 2011),以及～1.78Ga嵩山地区的A型花岗岩(Zhao and Zhou, 2009；Zhang *et al.*, 2013)和～1.60Ga的龙王碾花岗岩(陆松年等, 2003；包志伟等, 2009；Wang *et al.*, 2012),它们主要沿着北缘的燕辽裂谷和南缘的熊耳裂谷分布。华北南缘的熊耳群和北缘的长城系都属于未变质火山-沉积地层,不整合覆盖在太古宇和古元古界变质基底上(Zhai and Liu, 2003),表现出裂谷系中发育A型花岗岩的特点(Zhai and Liu, 2003；Zhai and Santosh, 2011；Zhai *et al.*, 2011；翟明国等, 2014)。

最近我们在华北克拉通南缘洛南县麻坪镇发现的元古宙的花岗斑岩,与陕西蓝田张家坪花岗岩体(数据未发表)、栾川龙王碾花岗岩体(包志伟等, 2009；Wang *et al.*, 2012)位于同一条碱性岩-碱性花岗岩带上。本文将通过系统的锆石年代学和Hf同位素组成、岩石学和地球化学研究,以期揭示麻坪岩体的岩石成因及其整个华北克拉通在全球超级大陆演化中的地质意义。

2 岩体地质及岩相学特征

华北克拉通南缘分布一条碱性岩-碱性花岗岩带,该岩带西起陕西蓝田张家坪地区经洛南,河南卢氏、栾川,南召北部和方城等地,东到平顶山-舞阳地区,长度达400km(图1b)。龙王碾花岗岩体是该带中规模最大的碱性花岗岩侵入体,而本文研究的麻坪花岗岩体则是与龙王碾花岗岩体属于同一碱性花岗岩带上的产物。

麻坪岩体位于陕西省洛南县麻坪镇,属于华北克拉通南缘西南部(图1a)。研究区内出露的地层主要为中元古界官道口群的碳酸盐岩和碎屑岩,由老到新依次为:高山河组、龙家园组、巡检司组、杜关组和冯家湾组。

麻坪岩体主要沿着洛南县麻坪镇地区的四洼-师家沟分布,呈带状延展,走向北西西,与地层走向平行,带长约5km,宽500m(图1c)。岩石类型有花岗斑岩、正长斑岩、正长花岗岩和霓辉正长斑岩(地矿部陕西地勘局, 1988；柳晓艳, 2011),但是由于岩体多被第四系覆盖且受地形所限,本文仅发现花岗斑岩,出露宽度约50m,侵位于官道口群龙家园组碳酸盐岩中(图1c)。

麻坪岩体花岗斑岩具斑状结构,块状构造,斑晶主要为钾长石和石英(图2a-d)。钾长石斑晶多为肉红色,呈板状、长柱状,自形,颗粒较大(1～2cm),约占33%；石英斑晶多呈浑圆状,粒径0.25～2.2mm,约占10%。基质也主要由钾长石和石英组成,呈浅绿色,含量约52%。钾长石和石英斑晶通常被熔蚀呈蠕虫状、港湾状和浑圆状,在边部还可见窄的熔蚀反应边(图2d),熔蚀现象指示麻坪花岗斑岩形成于浅成环境。斑晶周围常可见钾长石和石英形成的显微文象结构,基质呈显微晶质结构和球粒结构(图2f),可能与近地表快速冷凝的条件下固结有关。此外,还有少量黑云母(2%)(图2e),其蚀变较为强烈,部分完全蚀变为绢云母。部分钾长石发生绢云母化(图2e, f)、碳酸盐化、泥化。副矿物有磁铁矿、锆石、电气石等,含量约3%。

3 测试方法

锆石用常规方法分选,双目镜下挑纯,选取晶形较好、具代表性的锆石粘贴在环氧树脂表面,抛光后将待测锆石进行阴极发光(CL)图像分析。锆石的制靶和CL照相在中国科学院广州地球化学研究所同位素地球化学国家重点实验室完成。锆石U-Pb测年分析在合肥工业大学资源与环境工程学院完成,采用的仪器型号为Agilent 7500a,激光剥蚀系统为Coherent Inc公司生产的ComPex102 ArF准分子激光剥蚀系统。分析时激光束斑直径为32μm,激光脉冲重复频率为6Hz。实验原理和详细的测试方法见闫峻等(2012)。

锆石U-Pb年龄测定后,再在原位用LA-MC-ICP-MS进行Lu-Hf同位素分析,测试在中国科学院广州地球化学研究所同位素地球化学国家重点实验室完成。Lu-Hf同位素测试使用Thermo公司制造的Neptune型多接收电感耦合等离子体质谱(LA-MC-ICP-MS),加载德国Lamda Physik公司制造的Geolas 193nm准分子激光取样系统。激光束直径为32μm,剥蚀频率为8Hz,能量密度为15～20J/cm^2,剥蚀时间约60s。详细的分析程序见Wu *et al.*(2006)。

全岩的主微量元素分别在中国科学院广州地球化学研究所同位素地球化学国家重点实验室Rigaku ZSX 100e型荧光光谱仪(XRF)、PE Elan 6000型电感耦合等离子体-质谱仪(ICP-MS)上完成。详细分析见刘颖等(1996)。

4 测试结果

4.1 锆石U-Pb年龄

本文对麻坪岩体中的2个花岗斑岩样品进行了LA-ICPMS锆石U-Pb定年,分别是13MP-6(N 34°09′22.77″, E 110°02′40.71″,图1c)和13MP-9(N 34°09′04.77″, E 110°

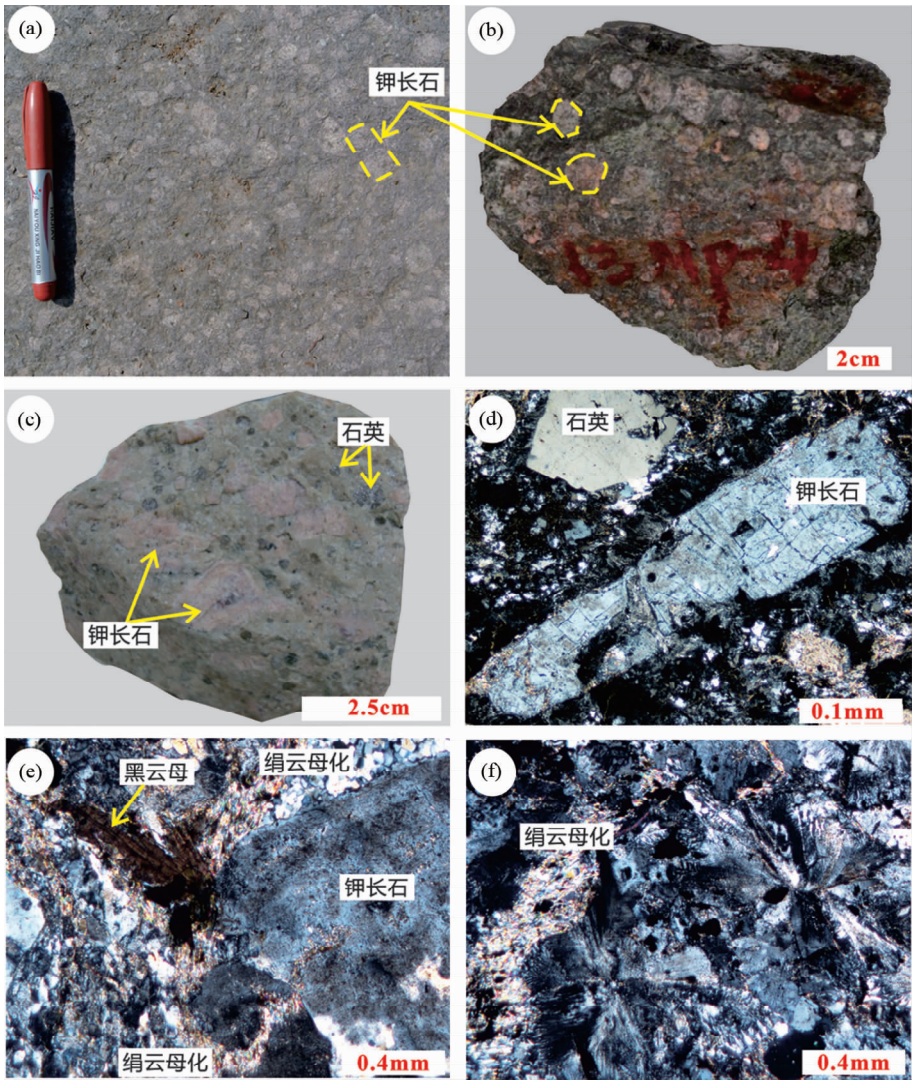

图 2 麻坪花岗斑岩手标本(a-c)及显微(d-f)照片

Fig. 2 Hand specimens (a-c) and micrographs (d-f) of the Maping granite porphyry

02′01.55″)。锆石多为无色透明-半透明,呈长柱状或椭圆状,自形程度较好,粒径在 70 ~ 200μm 之间,长宽比值范围为 1∶1 ~ 2∶1,振荡环带结构明显(图 3)。锆石的 Th/U 比值为 0.6 ~ 1.4,与典型的岩浆锆石特征相似(Belousova *et al.*, 2002)。LA-ICPMS 锆石 U-Pb 测年分析结果见表 1。

其中,样品 13MP-6 进行了 28 个测点的分析,$^{207}Pb/^{206}Pb$ 年龄集中于 1502 ~ 1702Ma,在谐和线图上(图 4a),样品的 28 个测点均分布在谐和线上或其附近,交点年龄为 1607 ± 32Ma(MSWD = 0.28),加权平均年龄为 1600 ± 24Ma(MSWD = 0.65)。样品 13MP-9 进行了 22 个测点的分析,$^{207}Pb/^{206}Pb$ 年龄变化于 1461 ~ 1694Ma 之间,各点均位于谐和线上或者靠近谐和线,给出的交点年龄为 1597 ± 67Ma(MSWD = 0.46),与加权平均年龄 1583 ± 28Ma 一致(图 4b)。两者在误差范围内一致,代表了岩体的形成时代(~1600Ma)。该年龄与柳晓艳(2011)获得的 1598 ± 9Ma(SHRIMP 锆石 U-Pb 年龄,样品号 07-5-1)正长花岗岩的形成年龄也一致,明显不同于前人获得的容易受到后期热扰动的 Rr-Sr 等时线年龄(约 524Ma,地矿部陕西地勘局,1998)。

4.2 全岩主-微量元素

麻坪花岗斑岩的主-微量元素含量列于表 2。所有样品具有高硅(SiO_2 = 70.51% ~ 75.69%)、富碱($K_2O + Na_2O$ = 9.00% ~ 10.27%)、高 K_2O/Na_2O 比值(>23)以及低 MgO(0.24% ~ 0.58%)、CaO(0.06% ~ 0.12%)、P_2O_5(0.04% ~ 0.08%)和 MnO(0.01%)的特征。在 TAS 图解中落于花岗岩区域(图 5a)。它们高的 A/NK(>1.13)和 A/CNK(>1.11)值,落在强过铝质花岗岩的区域(图 5b)。在 Harker 图解中,SiO_2 与 $Fe_2O_3^T$ 显示明显的负相关性,而与 Al_2O_3、MgO 和 TiO_2 呈现弱的负相关(图 6)。

花岗斑岩稀土元素总量(∑REE)较高,为 465.3×10^{-6}

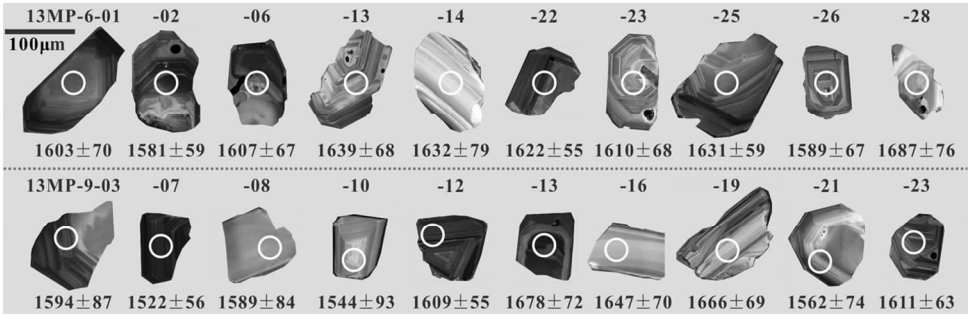

图3 麻坪岩体锆石阴极发光图像

Fig. 3 Zircon cathodoluminescence images from the Maping granite porphyry

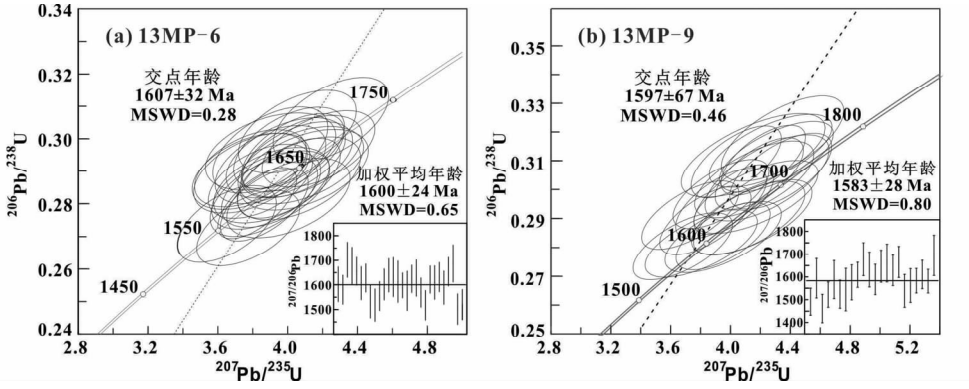

图4 麻坪花岗斑岩锆石 LA-ICP-MS U-Pb 谐和年龄图

Fig. 4 U-Pb concordia diagrams of zircons from the Maping granite porphyry

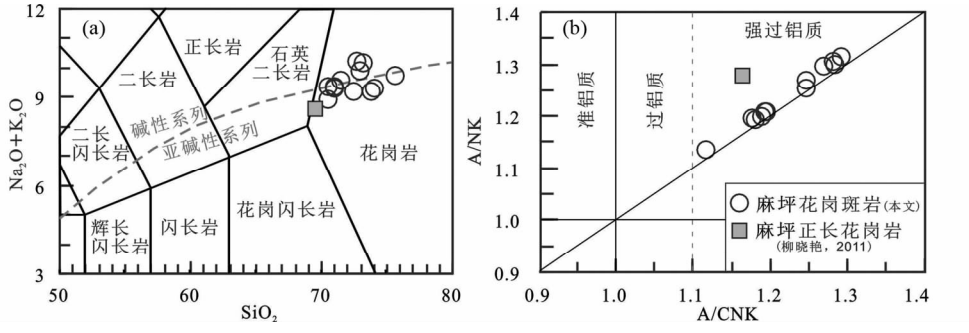

图5 麻坪花岗斑岩 TAS 图(a,据 Wilson, 1989)和 ACNK-ANK 图(b,据 Maniar and Piccoli, 1989)

Fig. 5 Classification plots of SiO_2 vs. ($Na_2O + K_2O$) (a, after Wilson, 1989) and A/CNK vs. A/NK (b, after Maniar and Piccoli, 1989) for the Maping granite porphyry

~848.7×10^{-6}(表2)。在球粒陨石标准化稀土分布模式图上,所有样品显示出相似的平滑右倾型特征,轻重稀土分异明显($(La/Yb)_{CN}$ = 13.2 ~ 17.68),具有弱的重稀土的亏损($(Gd/Yb)_{CN}$ = 1.43 ~ 3.05)以及明显的 Eu 负异常(δEu = 0.33 ~ 0.55),与正长花岗岩的曲线特征一致(柳晓艳,2011),而整体位于龙王磡花岗岩的稀土配分模式图下方(图7a)。在微量元素蛛网图上,所有花岗斑岩样品显示出明显的大离子亲石元素(LILE)的富集以及 Ba、Sr、Ti、Nb、Ta、Zr 和 Hf 等元素的亏损(图7b)。

4.3 锆石 Lu-Hf 同位素组成

锆石 Lu-Hf 同位素组成列于表3。麻坪花岗斑岩的锆石显示变化范围较大的$^{176}Hf/^{177}Hf$ 初始比值(0.281334 ~ 0.281615),平均值为 0.281537;对应的 $\varepsilon_{Hf}(t=1600Ma)$ 值介于 -16.7 ~ -6.9,主要集中在 -11.1 ~ -6.9。二阶段模式年龄(t_{DM}^{C})主要集中于 2767 ~ 3381Ma。在 $\varepsilon_{Hf}(t)$-t 图中(图8),样品的原位 Hf 同位素分析数据点均投影于球粒陨石 Hf 同位素演化线之下。

表 1 麻坪岩体锆石 LA-ICP-MS 分析结果

Table 1 LA-ICP-MS zircon U-Pb results for the Maping granite porphyry

测点号	Th ($\times10^{-6}$)	U ($\times10^{-6}$)	Th/U	同位素比值						年龄(Ma)					
				$\frac{^{207}Pb}{^{206}Pb}$	$\pm1\sigma$	$\frac{^{207}Pb}{^{235}U}$	$\pm1\sigma$	$\frac{^{206}Pb}{^{238}U}$	$\pm1\sigma$	$\frac{^{207}Pb}{^{206}Pb}$	$\pm1\sigma$	$\frac{^{207}Pb}{^{235}U}$	$\pm1\sigma$	$\frac{^{206}Pb}{^{238}U}$	$\pm1\sigma$
13MP-6-01	38.0	41.9	0.9	0.0989	0.0037	3.9892	0.2256	0.2941	0.0082	1603	70.4	1632	46.0	1662	40.6
13MP-6-02	67.5	90.4	0.7	0.0977	0.0030	4.0077	0.2096	0.2972	0.0083	1581	58.8	1636	42.5	1677	41.2
13MP-6-03	27.4	29.0	0.9	0.1043	0.0043	4.0641	0.2333	0.2878	0.0084	1702	71.5	1647	46.8	1631	42.1
13MP-6-04	47.2	41.7	1.1	0.1029	0.0042	4.0936	0.2432	0.2905	0.0082	1677	75.6	1653	48.5	1644	40.9
13MP-6-05	102	114	0.9	0.1011	0.0031	4.0750	0.2377	0.2918	0.0079	1656	56.9	1649	47.6	1651	39.2
13MP-6-06	58.6	98.1	0.6	0.0991	0.0033	3.9071	0.2185	0.2857	0.0076	1607	66.8	1615	45.2	1620	38.3
13MP-6-07	63.2	103	0.6	0.1002	0.0031	3.9308	0.2049	0.2845	0.0077	1628	56.8	1620	42.2	1614	38.8
13MP-6-08	36.8	49.7	0.7	0.0953	0.0034	3.9005	0.2179	0.2965	0.0088	1533	66.8	1614	45.2	1674	43.6
13MP-6-10	47.0	47.2	1.0	0.0945	0.0035	3.7942	0.2198	0.2894	0.0081	1518	65.7	1592	46.6	1639	40.5
13MP-6-11	77.3	108	0.7	0.0963	0.0030	3.8439	0.1968	0.2869	0.0075	1555	58.8	1602	41.3	1626	37.6
13MP-6-12	64.9	74.7	0.9	0.0988	0.0033	4.0291	0.1943	0.2956	0.0080	1602	63.0	1640	39.3	1670	39.7
13MP-6-13	42.2	45.7	0.9	0.1008	0.0037	4.0076	0.1942	0.2879	0.0081	1639	67.7	1636	39.4	1631	40.5
13MP-6-14	38.1	32.5	1.2	0.1004	0.0043	3.7738	0.1948	0.2725	0.0076	1632	79.2	1587	41.5	1554	38.5
13MP-6-15	22.2	27.0	0.8	0.0994	0.0045	3.8634	0.2031	0.2823	0.0081	1613	83.8	1606	42.4	1603	40.9
13MP-6-16	328	280	1.2	0.0986	0.0027	3.8254	0.1490	0.2802	0.0072	1598	50.6	1598	31.4	1592	36.1
13MP-6-17	29.9	27.3	1.1	0.0974	0.0041	3.6516	0.1869	0.2738	0.0077	1576	79.6	1561	40.8	1560	39.1
13MP-6-18	118	108	1.1	0.1000	0.0030	3.8663	0.1662	0.2797	0.0073	1624	55.6	1607	34.7	1590	36.8
13MP-6-19	47.1	44.4	1.1	0.1002	0.0040	4.0834	0.2262	0.2946	0.0083	1628	73.8	1651	45.2	1664	41.3
13MP-6-20	52.7	82.4	0.6	0.0971	0.0030	3.9018	0.2094	0.2920	0.0079	1569	59.3	1614	43.4	1652	39.6
13MP-6-21	84.7	89.8	0.9	0.0945	0.0030	3.7828	0.2176	0.2900	0.0077	1518	59.7	1589	46.2	1641	38.6
13MP-6-22	124	133	0.9	0.0999	0.0030	4.0529	0.2108	0.2935	0.0077	1622	55.1	1645	42.4	1659	38.5
13MP-6-23	61.0	57.3	1.1	0.0992	0.0036	3.8769	0.2062	0.2841	0.0078	1610	67.7	1609	43.0	1612	39.2
13MP-6-25	60.1	79.9	0.8	0.1003	0.0032	4.2474	0.2185	0.3058	0.0087	1631	59.3	1683	42.3	1720	42.9
13MP-6-26	66.2	65.3	1.0	0.0976	0.0035	4.0554	0.2230	0.3022	0.0084	1589	67.3	1645	44.8	1702	41.8
13MP-6-27	119	107	1.1	0.1015	0.0032	4.1764	0.2131	0.2969	0.0078	1654	57.9	1669	41.8	1676	38.7
13MP-6-28	29.6	36.8	0.8	0.1035	0.0042	4.0045	0.2333	0.2818	0.0080	1687	75.5	1635	47.4	1600	40.5
13MP-6-29	75.0	91.7	0.8	0.0936	0.0028	3.7875	0.2119	0.2909	0.0078	1502	62.0	1590	45.0	1646	39.1
13MP-6-30	62.0	92.8	0.7	0.0946	0.0031	3.9019	0.2466	0.2960	0.0079	1520	61.1	1614	51.1	1672	39.1
13MP-9-02	65.7	81.4	0.8	0.0932	0.0029	4.0355	0.1998	0.3098	0.0082	1491	59.3	1641	40.3	1740	40.4
13MP-9-03	21.5	23.0	0.9	0.0984	0.0046	4.3464	0.2715	0.3179	0.0098	1594	87.0	1702	51.6	1779	47.8
13MP-9-06	90.4	141	0.6	0.0916	0.0030	3.7250	0.2164	0.2914	0.0077	1461	62.2	1577	46.5	1649	38.7
13MP-9-07	90.4	117	0.8	0.0942	0.0028	3.9329	0.2130	0.2987	0.0079	1522	55.6	1620	43.9	1685	39.0
13MP-9-08	28.4	27.6	1.0	0.0981	0.0044	4.1549	0.2643	0.3038	0.0087	1589	83.6	1665	52.1	1710	43.2
13MP-9-09	72.0	83.9	0.9	0.0948	0.0031	3.6758	0.2208	0.2807	0.0076	1524	61.9	1566	48.0	1595	38.4
13MP-9-10	18.9	19.8	1.0	0.0953	0.0048	4.1485	0.3203	0.3121	0.0095	1544	93.4	1664	63.2	1751	46.9
13MP-9-11	43.2	45.5	0.9	0.0974	0.0038	3.8000	0.2489	0.2816	0.0077	1576	76.9	1593	52.7	1599	38.6
13MP-9-12	75.0	131	0.6	0.0991	0.0029	4.3042	0.2529	0.3115	0.0081	1609	55.2	1694	48.4	1748	39.7
13MP-9-13	95.8	109	0.9	0.1024	0.0040	4.1398	0.2670	0.2908	0.0085	1678	72.2	1662	52.8	1645	42.3
13MP-9-14	51.3	42.8	1.2	0.1004	0.0042	3.9468	0.2583	0.2839	0.0080	1632	76.7	1623	53.1	1611	40.4
13MP-9-15	69.4	66.4	1.0	0.0976	0.0035	4.2662	0.2724	0.3137	0.0084	1589	66.7	1687	52.6	1759	41.1
13MP-9-16	62.5	44.9	1.4	0.1012	0.0039	4.1678	0.2752	0.2977	0.0083	1647	70.4	1668	54.1	1680	41.1
13MP-9-17	17.7	21.0	0.8	0.1020	0.0046	4.2431	0.2752	0.3043	0.0098	1661	83.2	1682	53.3	1713	48.5
13MP-9-18	126	98.0	1.3	0.1003	0.0034	3.9466	0.2092	0.2841	0.0077	1629	67.1	1623	43.0	1612	38.5
13MP-9-19	34.9	39.2	0.9	0.1023	0.0038	4.3347	0.2259	0.3066	0.0086	1666	68.5	1700	43.0	1724	42.7
13MP-9-20	56.5	50.4	1.1	0.0955	0.0037	3.8275	0.2029	0.2896	0.0078	1539	72.2	1599	42.7	1639	39.0
13MP-9-21	63.2	51.7	1.2	0.0967	0.0038	3.9328	0.2023	0.2954	0.0080	1562	74.1	1620	41.7	1669	39.6
13MP-9-22	185	149	1.2	0.0977	0.0028	4.0188	0.1773	0.2968	0.0079	1583	53.7	1638	35.9	1675	39.1
13MP-9-23	69.7	91.1	0.8	0.0993	0.0033	4.1903	0.1961	0.3058	0.0082	1611	62.5	1672	38.4	1720	40.4
13MP-9-24	172	241	0.7	0.0977	0.0027	4.2147	0.1875	0.3104	0.0080	1581	51.8	1677	36.5	1742	39.4
13MP-9-25	30.3	26.3	1.2	0.1038	0.0050	4.1219	0.2473	0.2904	0.0084	1694	88.3	1659	49.1	1643	41.9

表2 麻坪岩体主量(wt%)和微量元素($\times10^{-6}$)分析结果

Table 2 Major (wt%) and trace element concentrations ($\times10^{-6}$) of the Maping pluton

样品号	13MP-1	13MP-2	13MP-3	13MP-4	13MP-5	13MP-6	13MP-7	13MP-9	13MP-10	13MP-11	13MP-12	13MP-13	07-5-1
岩性	花岗斑岩												正长花岗岩
SiO_2	75.69	71.04	72.47	70.51	73.19	71.56	72.80	74.04	70.58	73.86	71.03	73.00	69.71
TiO_2	0.36	0.46	0.45	0.40	0.44	0.39	0.36	0.31	0.35	0.25	0.46	0.33	0.40
Al_2O_3	12.21	13.39	13.48	12.93	13.40	12.78	13.61	12.89	13.38	12.09	13.01	13.13	13.89
$Fe_2O_3^T$	0.56	3.43	2.12	5.14	0.81	3.65	1.16	1.65	3.98	2.86	4.10	2.08	4.76
MnO	0.01	0.01	0.01	0.01	0.01	0.01	0.01	0.01	0.01	0.01	0.01	0.01	0.08
MgO	0.24	0.55	0.51	0.45	0.50	0.48	0.42	0.39	0.58	0.39	0.53	0.31	0.86
CaO	0.11	0.12	0.11	0.10	0.10	0.09	0.08	0.06	0.07	0.06	0.11	0.07	0.57
Na_2O	0.21	0.22	0.38	0.26	0.19	0.21	0.22	0.19	0.18	0.13	0.19	0.26	2.75
K_2O	9.61	9.18	8.87	8.73	10.05	9.43	10.05	9.17	9.22	9.14	9.16	9.68	5.86
P_2O_5	0.07	0.08	0.07	0.07	0.07	0.05	0.05	0.04	0.05	0.05	0.06	0.05	0.09
LOI	0.60	1.15	1.19	1.05	0.88	0.99	0.90	0.91	1.25	0.81	0.99	0.73	1.70
Total	99.65	99.64	99.65	99.66	99.65	99.65	99.65	99.66	99.65	99.64	99.65	99.65	100.67
$Mg^{\#}$	50.3	27.4	35.8	16.8	58.8	23.4	45.8	35.5	25.3	24.1	23.2	25.8	38.38
K_2O+Na_2O	9.81	9.40	9.24	9.00	10.24	9.64	10.27	9.36	9.40	9.27	9.35	9.95	8.61
K_2O/Na_2O	46.7	42.1	23.5	33.0	53.3	44.4	46.7	47.7	51.7	68.7	48.7	37.0	2.13
A/NK	1.13	1.30	1.32	1.31	1.19	1.21	1.21	1.26	1.30	1.19	1.27	1.20	1.28
A/CNK	1.11	1.26	1.28	1.27	1.17	1.18	1.19	1.24	1.28	1.17	1.24	1.18	1.13
T_{Zr}(℃)	871	953	942	935	942	916	923	873	923	870	939	904	925
Ga	14.2	22.8	22.1	22.5	22.8	22.2	24.0	22.8	22.6	18.0	22.2	23.1	24.6
Rb	124	165	139	161	173	185	185	148	180	110	163	178	164
Sr	14.3	22.0	26.8	19.7	14.2	13.0	15.9	15.9	12.1	16.2	16.1	17.8	87.0
Y	51.0	52.3	61.2	49.7	52.4	48.9	56.6	55.7	58.7	57.6	47.6	57.3	57.3
Zr	344	671	595	570	648	514	539	319	513	325	606	456	596
Nb	36.3	45.0	42.1	38.6	45.0	37.4	38.9	–	35.6	35.1	42.8	35.1	45.1
Cs	1.07	1.29	1.31	1.26	1.01	0.79	0.88	1.29	1.51	1.59	1.27	1.05	6.76
Ba	487	994	875	1060	787	951	1323	718	1198	365	891	1355	1918
Hf	9.84	16.4	15.0	14.2	16.5	13.4	13.7	9.41	13.1	9.50	15.2	11.9	18.0
Ta	2.30	2.44	2.45	2.25	2.73	2.28	2.35	0.10	2.11	2.26	2.44	2.22	2.02
Pb	4.47	6.02	3.84	8.41	3.19	5.74	4.54	4.73	8.90	4.93	6.10	4.76	39.9
Th	29.2	26.3	28.2	26.2	32.0	26.0	28.7	31.7	24.3	30.9	28.3	27.0	21.3
U	1.61	1.60	1.63	2.05	3.08	1.83	2.04	1.96	1.99	1.65	1.49	1.57	2.62
La	127	112	128	123	127	116	135	154	128	153	99	132	148
Ce	264	220	254	253	240	230	263	299	252	363	206	256	273
Pr	30.1	26.5	30.7	29.2	26.2	27.5	31.4	35.1	29.6	51.3	24.6	31.0	31.5
Nd	106	94.7	110	104	89.8	97.1	111	123	105	191	85.2	110	109
Sm	16.0	14.7	16.8	15.8	13.7	14.8	17.0	19.1	16.0	31.9	13.4	17.0	17.7
Eu	1.51	2.42	2.21	2.30	2.09	2.09	2.41	1.94	2.38	3.41	1.89	2.24	2.75
Gd	11.9	12.2	12.9	12.3	11.3	12.3	13.8	14.8	13.4	22.9	10.3	13.7	15.1
Tb	1.67	1.74	1.97	1.77	1.65	1.74	1.92	1.99	1.96	2.60	1.56	1.94	2.02
Dy	9.58	10.2	11.7	10.1	10.0	10.1	11.1	11.3	11.4	12.6	9.18	11.0	11.2
Ho	1.95	2.12	2.42	2.05	2.16	2.06	2.30	2.30	2.35	2.40	1.92	2.26	2.27
Er	5.44	5.95	6.58	5.50	6.27	5.56	6.38	6.35	6.34	6.46	5.35	6.13	6.43
Tm	0.82	0.91	0.98	0.82	0.98	0.84	0.95	0.96	0.94	0.96	0.81	0.90	0.93
Yb	5.34	5.92	6.26	5.29	6.57	5.41	6.14	6.16	6.00	6.21	5.40	5.72	5.96
Lu	0.83	0.92	0.98	0.84	1.02	0.84	0.96	0.93	0.92	0.94	0.86	0.89	0.91
∑REE	582	510	586	565	539	526	603	677	576	849	465	591	627
$(La/Yb)_{CN}$	17.0	13.5	14.7	16.7	13.9	15.3	15.8	18.0	15.2	17.7	13.2	16.6	17.8
δEu	0.32	0.54	0.44	0.49	0.50	0.46	0.47	0.34	0.48	0.37	0.47	0.43	0.5

注：样品07-5-1据柳晓艳(2011)；–代表未检测到；$Fe_2O_3^T$为全铁；$ACNK = Al_2O_3/(CaO+Na_2O+K_2O)$(摩尔比)；$ANK = Al_2O_3/(Na_2O+K_2O)$(摩尔比)；$Mg^{\#} = 100\times MgO/(MgO+FeO)$；$\delta Eu = (Eu/0.058)/SQRT((Sm/0.153)\times(Gd/0.206))$；$(La/Yb)_{CN}$为球粒陨石标准化值，标准化值引自 Sun and McDonough(1989)；T_{Zr}为锆石饱和温度，公式据 Miller *et al.* (2003)

表 3 麻坪岩体锆石 Hf 同位素组成

Table 3 LA-MC-ICP-MS zircon Hf isotopic compositions of the Maping granite porphyry

Spot No.	t(Ma)	$^{176}Yb/^{177}Hf$	$^{176}Lu/^{177}Hf$	$^{176}Hf/^{177}Hf$	$\pm 2\sigma$	$\varepsilon_{Hf}(0)$	$\varepsilon_{Hf}(t)$	t_{DM1}(Ma)	t_{DM}^{C}(Ma)	$f_{Lu/Hf}$
13MP-6-1		0.018548	0.000562	0.281559	0.000010	-42.9	-8.0	2344	2834	-0.98
13MP-6-2		0.017641	0.000563	0.281502	0.000010	-44.9	-10.0	2421	2961	-0.98
13MP-6-3		0.021114	0.000647	0.281537	0.000009	-43.7	-8.8	2379	2888	-0.98
13MP-6-4		0.033333	0.000959	0.281525	0.000010	-44.1	-9.6	2415	2936	-0.97
13MP-6-6		0.017170	0.000501	0.281548	0.000009	-43.3	-8.3	2355	2854	-0.98
13MP-6-7		0.019387	0.000579	0.281540	0.000009	-43.6	-8.7	2372	2879	-0.98
13MP-6-8		0.014281	0.000426	0.281533	0.000009	-43.8	-8.8	2372	2884	-0.99
13MP-6-10		0.046078	0.001428	0.281615	0.000012	-40.9	-6.9	2320	2767	-0.96
13MP-6-11		0.019991	0.000577	0.281512	0.000010	-44.5	-9.6	2409	2940	-0.98
13MP-6-13		0.014810	0.000459	0.281527	0.000009	-44.0	-9.0	2382	2899	-0.99
13MP-6-14	1600	0.027183	0.000820	0.281555	0.000010	-43.1	-8.4	2366	2862	-0.98
13MP-6-15		0.018904	0.000557	0.281559	0.000012	-42.9	-8.0	2344	2834	-0.98
13MP-6-17		0.027309	0.000814	0.281569	0.000010	-42.6	-7.9	2346	2830	-0.98
13MP-6-18		0.035014	0.001009	0.281497	0.000012	-45.1	-10.7	2457	3004	-0.97
13MP-6-20		0.020344	0.000585	0.281511	0.000012	-44.6	-9.7	2410	2942	-0.98
13MP-6-21		0.026836	0.000821	0.281478	0.000012	-45.8	-11.1	2470	3033	-0.98
13MP-6-22		0.024358	0.000696	0.281539	0.000011	-43.6	-8.8	2380	2889	-0.98
13MP-6-23		0.033769	0.001028	0.281484	0.000017	-45.5	-11.1	2476	3033	-0.97
13MP-6-25		0.018137	0.000545	0.281546	0.000011	-43.3	-8.4	2360	2861	-0.98
13MP-6-26		0.019200	0.000571	0.281503	0.000009	-44.9	-10.0	2421	2961	-0.98
13MP-6-27		0.039369	0.001230	0.281334	0.000019	-50.9	-16.7	2695	3381	-0.96
13MP-6-28		0.015151	0.000456	0.281580	0.000010	-42.2	-7.1	2310	2781	-0.99
13MP-9-3		0.015053	0.000469	0.281582	0.000009	-42.1	-7.1	2308	2777	-0.99
13MP-9-6		0.017593	0.000519	0.281579	0.000009	-42.2	-7.2	2315	2787	-0.98
13MP-9-7		0.025061	0.000726	0.281544	0.000008	-43.4	-8.7	2375	2880	-0.98
13MP-9-8		0.024649	0.000737	0.281546	0.000009	-43.4	-8.6	2373	2875	-0.98
13MP-9-9		0.020740	0.000599	0.281561	0.000009	-42.8	-7.9	2344	2832	-0.98
13MP-9-10		0.029851	0.000897	0.281566	0.000011	-42.7	-8.1	2356	2842	-0.97
13MP-9-12		0.017185	0.000522	0.281542	0.000008	-43.5	-8.5	2365	2869	-0.98
13MP-9-13	1600	0.018930	0.000548	0.281545	0.000008	-43.4	-8.5	2363	2865	-0.98
13MP-9-14		0.026482	0.000770	0.281537	0.000009	-43.7	-9.0	2387	2897	-0.98
13MP-9-16		0.037434	0.001079	0.281543	0.000009	-43.5	-9.1	2398	2905	-0.97
13MP-9-17		0.015416	0.000489	0.281571	0.000009	-42.5	-7.5	2324	2803	-0.99
13MP-9-19		0.024722	0.000660	0.281496	0.000009	-45.1	-10.3	2436	2982	-0.98
13MP-9-21		0.031839	0.000914	0.281542	0.000009	-43.5	-8.9	2389	2896	-0.97
13MP-9-22		0.045758	0.001268	0.281545	0.000009	-43.4	-9.2	2407	2913	-0.96
13MP-9-23		0.026013	0.000752	0.281504	0.000008	-44.8	-10.1	2430	2969	-0.98
13MP-9-24		0.055407	0.001495	0.281546	0.000009	-43.4	-9.4	2420	2927	-0.95

注: $\varepsilon_{Hf}(0) = ((^{176}Hf/^{177}Hf)_S/(^{176}Hf/^{177}Hf)_{CHUR,0} - 1) \times 10000$; $\varepsilon_{Hf}(t) = ((^{176}Hf/^{177}Hf)_S - (^{176}Lu/^{177}Hf)_S \times (e^{\lambda t} - 1))/((^{176}Hf/^{177}Hf)_{CHUR,0} - (^{176}Lu/^{177}Hf)_{CHUR} \times (e^{\lambda t} - 1)) - 1) \times 10000$; t_{DM1}(Ma) $= 1/\lambda \times \ln(1 + ((^{176}Hf/^{177}Hf)_S - (^{176}Hf/^{177}Hf)_{DM})/((^{176}Lu/^{177}Hf)_S - (^{176}Lu/^{177}Hf)_{DM}))$; t_{DM}^{C}(Ma) $= t_{DM1} - (t_{DM1} - t)((f_{CC} - f_S)/(f_{CC} - f_{DM}))$; $f_{Lu/Hf} = (^{176}Lu/^{177}Hf)_S/(^{176}Lu/^{177}Hf)_{CHUR} - 1$, $(^{176}Lu/^{177}Hf)_S$ 和 $(^{176}Hf/^{177}Hf)_S$ 是样品的测定值; $(^{176}Lu/^{177}Hf)_{CHUR} = 0.03321$ 和 $(^{176}Hf/^{177}Hf)_{CHUR,0} = 0.282772$ (Blichert-Toft and Albarède, 1997); $(^{176}Lu/^{177}Hf)_{DM} = 0.03842$ 和 $(^{176}Hf/^{177}Hf)_{DM} = 0.28325$ (Griffin *et al.*, 2000), t = 锆石结晶年龄; $\lambda = 1.867 \times 10^{-11}\,y^{-1}$ (Söderlund *et al.*, 2004), $f_{Lu/Hf} = -0.55$ (Vervoort *et al.*, 1996)

5 讨论

5.1 岩石分类

在地球化学特征上,麻坪花岗斑岩具明显高的 Ga/Al 比值和 Zr + Nb + Ce + Y 含量(图 9),与典型的 A 型花岗岩的特征一致(Collins *et al.*, 1982; Whalen *et al.*, 1987; Frost and Frost, 2011)。其较高的 SiO_2 和 $K_2O + Na_2O$、低 CaO、MgO、P_2O_5、TiO_2 和 MnO,以及富集 K、Rb 等大离子亲石元素和亏损 Nb、Ta、Zr 和 Hf 等高场强元素和 Eu、Sr、Ti 等元素的特征

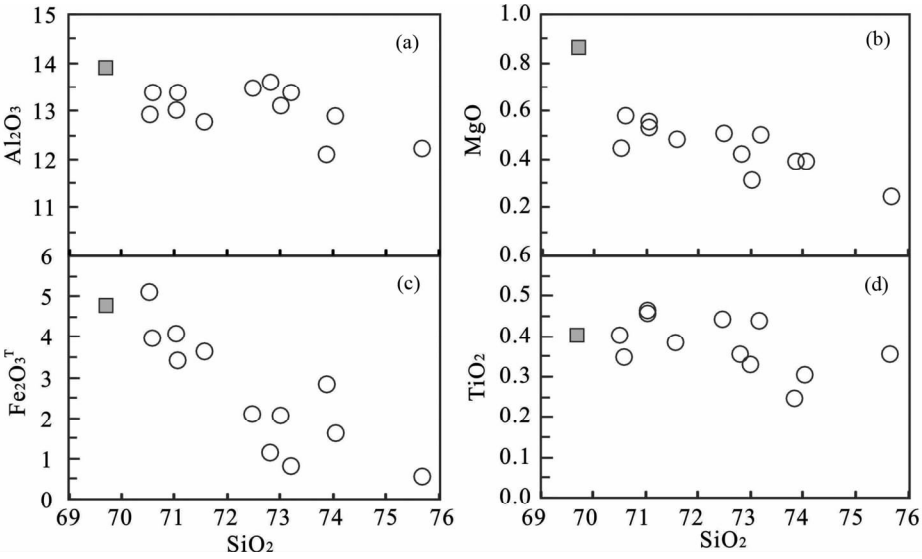

图 6 麻坪花岗斑岩 Harker 图解

Fig. 6 Harker variation diagrams for the Maping granite porphyry

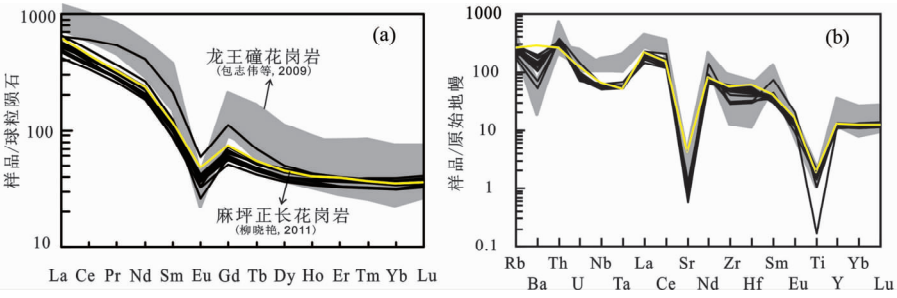

图 7 麻坪花岗斑岩球粒陨石标准化稀土元素配分图(a)和原始地幔标准化微量元素蛛网图(b)(标准化值得据 Sun and McDonough, 1989)

Fig. 7 Chondrite-normalized REE patterns (a) and primitive mantle-normalized spidergrams (b) of the Maping granite porphyry (normalized values after Sun and McDonough, 1989)

也与 A 型花岗岩相似。然而,它们较高的 A/CNK 值(> 1.11),显示为强过铝质花岗岩的特征,类似 S 型花岗岩(Martínez *et al.*, 2014)。与典型的 S 型花岗岩(一般具有高达 14% 的 Al_2O_3 和高含量的 P_2O_5,还含镁铁质岩浆岩包体(MMEs),King *et al.*, 2001; Bonin, 2004; Chen *et al.*, 2014)相比,麻坪花岗斑岩的 Al_2O_3(12% ~ 13.5%)和 P_2O_5(< 0.08%)均相对较低,并且结合野外地质和岩相学观察,未发现镁铁质包体。更为重要的是,其高的锆石饱和温度(Watson and Harrison, 1983)870 ~ 953℃(平均值为 915℃),与 A 型花岗岩形成温度非常相似(King *et al.*, 1997; Huang *et al.*, 2011),而明显高于 S 型花岗岩的形成温度(Cai *et al.*, 2011; Martínez *et al.*, 2014)。因此,这些花岗斑岩可归结为过铝质 A 型花岗岩。而事实上,该类 A 型花岗岩在我国华北南缘的鲁山地区(Zhou *et al.*, 2014)、塔里木克拉通北缘的库鲁克塔格地区(Long *et al.*, 2012)以及华南地区(Huang *et al.*, 2011; Zhao *et al.*, 2008)均有报道,说明具有过铝质特征的 A 型花岗岩并不少见。

5.2 岩石成因

目前关于 A 型花岗岩的成因主要有以下四种模型:①幔源碱性玄武岩的分异(Frost and Frost, 1997; Mushkin *et al.*, 2003);②继 I 型或者 S 型岩浆分异抽取之后的富含 F/Cl 的下地壳麻粒岩残留体的部分熔融(Collins *et al.*, 1982; Whalen *et al.*, 1987; King *et al.*, 1997, 2001);③壳-幔物质的混合作用(Kerr and Fryer, 1993; Mingram *et al.*, 2000; Yang *et al.*, 2006);④结晶基底或者变质沉积岩的部分熔融,并可能伴随有基性岩浆的底侵作用(Rämö *et al.*, 1995; Huang *et al.*, 2011; Long *et al.*, 2012; Zhou *et al.*, 2014)。其争议的焦点在于这类花岗岩是直接来自地幔玄武岩的分异,还是仅仅来自地壳、或者同时有地幔物质的加入(Wu *et al.*, 2002; Yang *et al.*, 2006; Bonin, 2007)。

麻坪 A 型花岗岩具有明显低的 $\varepsilon_{Hf}(t)$ 值和较大的二阶

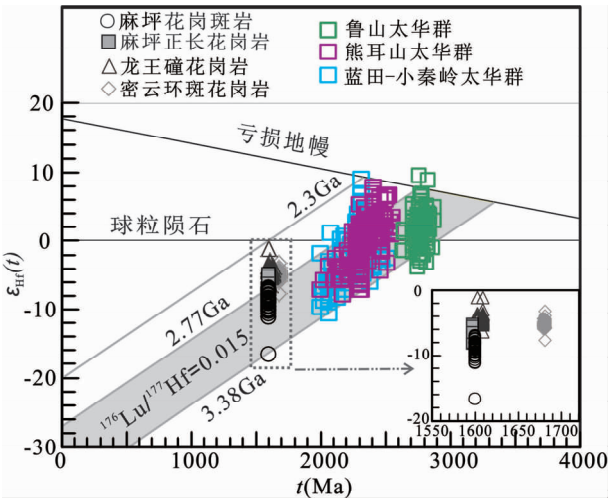

图 8 麻坪花岗斑岩 $\varepsilon_{Hf}(t)$-t 图解

麻坪正长花岗岩数据引自柳晓艳(2011),龙王磉花岗岩数据引自包志伟等(2009)、Wang *et al.* (2012),密云环斑花岗岩数据引自杨进辉等(2005),太华群数据引自 Liu *et al.* (2009)、Huang *et al.* (2010, 2012, 2013)、Xu *et al.* (2009)、第五春荣等(2007, 2010)、时毓等(2011)、Diwu *et al.* (2014)

Fig. 8 $\varepsilon_{Hf}(t)$ versus t diagram of the Maping granite porphyry

Maping syenogranite is from Liu (2011), Longwangzhuang granites are from Bao *et al.* (2009) and Wang *et al.* (2012), Miyun rapakivi granites are from Yang *et al.* (2005), Taihua group are form Liu *et al.* (2009), Huang *et al.* (2010, 2012, 2013), Xu *et al.* (2009), Shi *et al.* (2011) and Diwu *et al.* (2007, 2010, 2014)

段模式年龄(t_{DM}^{C}),表明这些 A 型花岗岩来源于古老的地壳。考虑到麻坪 A 型花岗岩具有高 K、Si、K/Na 比值以及明显的 Sr 负异常的特征,与继 I 型或者 S 型岩浆分异抽取之后的富含 F/Cl 的下地壳麻粒岩残留体的部分熔融形成的岩浆具有低 K、Si、K/Na 比值以及无 Sr 的负异常明显不同(Creaser *et al.*, 1991; Frost and Frost, 1997),很显然,具有该特征的下地壳残留体的部分熔融很难形成麻坪 A 型花岗岩。

在 $\varepsilon_{Hf}(t)$-*t* 图解中(图 8),麻坪花岗斑岩有较低的 $\varepsilon_{Hf}(t)$值(−16.7 ~ −6.9),t_{DM}^{C} = 2767 ~ 3381Ma,说明源区物质可能形成于 2767 ~ 3381Ma。与华北克拉通其他地区同时期富集地幔来源的 A 型花岗岩相比,如北缘的密云环斑花岗岩(~1683Ma, $\varepsilon_{Hf}(t)$ = −7.7 ~ −3.2, t_{DM}^{C} = 2.4 ~ 2.6Ga; Rämö *et al.*, 1995; 杨进辉等, 2005; 高维等, 2008)和南缘的龙王磉花岗岩(~1602Ma, $\varepsilon_{Hf}(t)$ = −1.11 ~ −5.26, t_{DM}^{C} = 2.6 ~ 2.8Ga; 包志伟等, 2009; Wang *et al.*, 2012),麻坪花岗斑岩具有明显低的 $\varepsilon_{Hf}(t)$值(图 8)和大的 t_{DM}^{C}值,说明麻坪花岗斑岩的源区与同期的密云环斑花岗岩和龙王磉花岗岩的源区不完全相同。

根据已有的研究数据显示,华北克拉通基底岩浆锆石的年龄峰值主要集中于 ~ 2.5Ga 和 2.8 ~ 2.7Ga,其中 ~ 2.5Ga 岩浆活动广泛存在于整个华北克拉通,而大面积 2.8 ~ 2.7Ga 的岩石年龄记录主要发现在河南鲁山、山东西部和胶东地区,代表了新太古代新生地壳的形成和少量古老地壳物质的再造(Liu *et al.*, 2009; 第五春荣等, 2010; Huang *et al.*, 2010, 2012; Zhang *et al.*, 2013)。华北克拉通南缘鲁山地区发育 2.8 ~ 2.7Ga 的 TTG 质片麻岩和斜长角闪岩,且在斜长角闪岩中存在 2.9Ga 甚至 3.1Ga 的残留锆石(Liu *et al.*, 2009; 第五春荣等, 2010),同时在熊耳山地区和蓝田-小秦岭地区分别发育有 2.5 ~ 2.0Ga、2.5 ~ 1.9Ga 的太华群物质(图 8; 第五春荣等, 2007; Xu *et al.*, 2009; 时毓等, 2011; Huang *et al.*, 2012, 2013; Diwu *et al.*, 2014),可能为麻坪花岗斑岩的形成提供了物质基础。此外,根据太华群变质岩中锆石 Hf 同位素数据(Liu *et al.*, 2009; Huang *et al.*, 2010, 2012, 2013; Xu *et al.*, 2009; 第五春荣等, 2007, 2010; 时毓等, 2011; Diwu *et al.*, 2014),其 $\varepsilon_{Hf}(t = 1600Ma)$的变化范围为 −30 ~ −7.18,包含麻坪岩体的同位素数据范围,表明麻坪 A 型花岗岩来自太华群的部分熔融(图 8)。

麻坪岩体相对较高的形成温度(>870℃)表明其形成与玄武质岩浆的底侵或者地幔柱活动有关(Frost and Frost, 1997; King *et al.*, 1997)。此外,岩石中 Al_2O_3、MgO、$Fe_2O_3^T$ 和 TiO_2 随着 SiO_2 含量的增加而减小(图 6),而 K_2O 随之而增大(图略),同时还有 Eu、Sr 和 Ti 负异常(图 7a, b),表明这些强过铝质岩浆在演化过程中经历了钾长石、斜长石、铁钛氧化物等的分离结晶作用。因此,麻坪岩体是由太华群高温条件下部分熔融形成的,这与 Eby (1992) 的 A_2 型花岗岩一致(图 10),同时基性岩浆的底侵作用为之提供了相应的热源。

5.3 地质意义

目前多数学者认为,华北克拉通在 ~ 1.8Ga 完成了克拉通化,此后未再遭受大规模的变质变形(Zhai and Liu, 2003; Zhai and Santosh, 2011; Zhai *et al.*, 2011; 翟明国等, 2014)。但是对于之后广泛发育的岩浆-沉积活动,包括多期次 A 型花岗岩、碱性岩和基性岩墙(Rämö *et al.*, 1995; 赵太平等, 2004; 杨进辉等, 2005; 任康绪等, 2006; Zhang *et al.*, 2007; 高维等, 2008; 包志伟等, 2009; Jiang *et al.*, 2011; 李怀坤等, 2011; Wang *et al.*, 2012, 2013),以及熊耳群和长城系火山-沉积建造(陆松年等, 2003; 李怀坤等, 1995; Zhao *et al.*, 2002; 赵太平等, 2004; Lu *et al.*, 2008),其构造背景一直存在争议。其争议的焦点在于是否是地幔柱(Zhai and Liu, 2003)、碰撞后(Wang *et al.*, 2004; Zhao and Zhou, 2009; Zhang *et al.*, 2013)或者大陆裂谷(Lu *et al.*, 2002; Hou *et al.*, 2008)作用的产物。

虽然如此,华北克拉通 ~ 1.68Ga 斜长岩-环斑花岗岩-正长岩等非造山岩浆组合的出现,表明此时的动力学背景是非造山伸展环境(Rämö *et al.*, 1995; 杨进辉等, 2005; 高维等, 2008; 包志伟等, 2009)。此外,在华北克拉通南缘沿着陕西蓝田张家坪 A 型花岗岩体(~ 1.52Ga,数据未发表)经

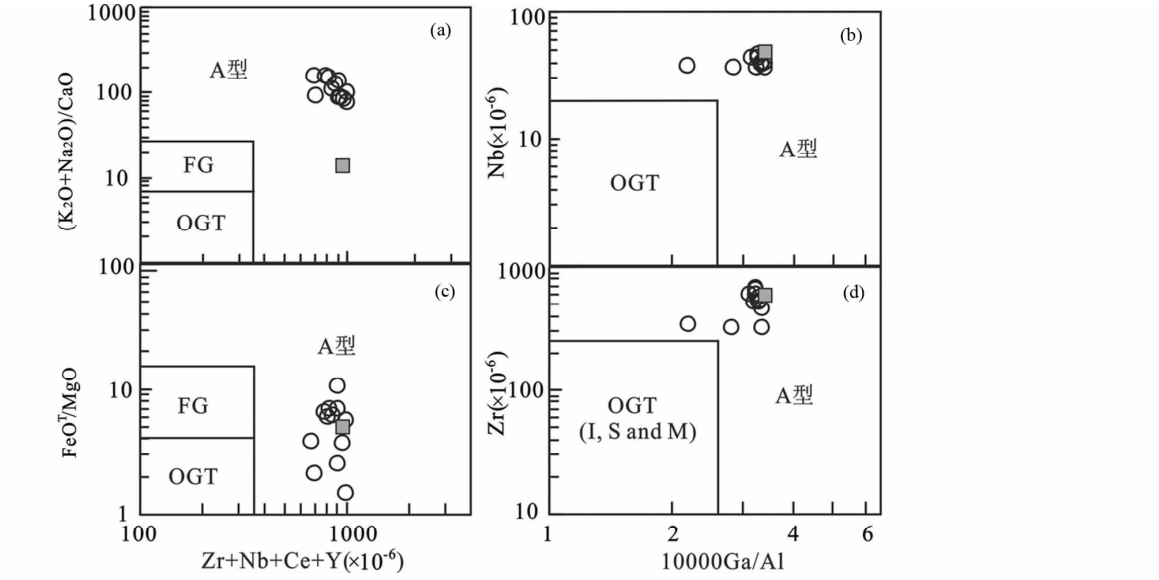

图9 A型花岗岩判别图解(据 Whalen *et al.*, 1987)

Fig. 9 Discrimination diagrams of A-type granite (after Whalen *et al.*, 1987)

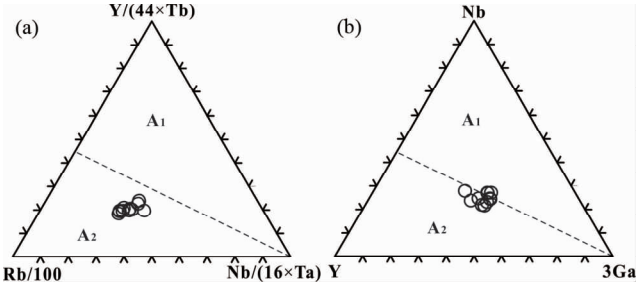

图10 麻坪岩体 Rb/100-Y/(44×Tb)-Nb/(16×Ta)(a)和 Y-Nb-3Ga(b)三角图解

A_1型代表来源于幔源熔体的分离结晶;A_2型代表来源于地壳部分熔融(据 Eby, 1992)

Fig. 10 Triangular plots of Rb/100-Y/(44×Tb)-Nb/(16×Ta) (a) and Y-Nb-3Ga (b) of the Maping A-type granites

The A_1-field is interpreted to indicate derivation via fractional crystallization of mantle-derived melts, whereas the A_2-field is interpreted to indicate derivation through partial melting of pre-existing crust (after Eby, 1992)

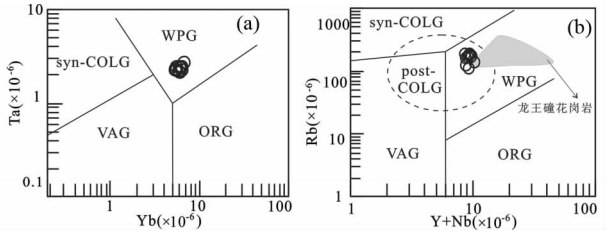

图11 麻坪花岗斑岩 Ta-Yb(a, Pearce *et al.*, 1984)和 Rb-(Yb+Ta)(b, 据 Pearce, 1986)构造图解

龙王磡花岗岩数据引自包志伟等(2009)和 Wang *et al.*(2012). WPG-板内花岗岩;ORG-洋脊花岗岩;VAG-火山弧花岗岩;syn-COLG and post-COLG-同碰撞/碰撞后花岗岩

Fig. 11 Discrimination diagrams of Ta-Yb (a, after Pearce *et al.*, 1984) and Rb-(Yb+Ta) (b, after Pearce, 1986) for tectonic settings of the Maping granitic porphyry

Field for Longwangzhuang granites is from Bao *et al.* (2009) and Wang *et al.* (2012). WPG: Within-Plate Granites; ORG: Ocean-Ridge Granites; VAG: Volcanic Arc Granites; syn-COLG and post-COLG: syn- and post-collisional Granites

洛南麻坪花岗斑岩(~1.6Ga,本文)到河南栾川龙王磡花岗岩体(~1.6Ga; 包志伟等, 2009; Wang *et al.*, 2012)分布着一条A型花岗岩带(图1b),说明伸展背景下岩浆活动的发育。同时,构造环境判别图解也显示,~1.6Ga龙王磡A型花岗岩都落在了板内的构造背景(图11)。虽然麻坪A型花岗岩落入板内和碰撞后环境的重叠区域,但是结合上述的区域地质背景资料,我们认为麻坪岩体仍形成于非造山的板内伸展环境。由此看来,华北克拉通中元古代裂谷作用导致地幔减压熔融形成基性岩浆,而基性岩浆的底侵作用提供了热源致使地壳发生部分熔融从而形成麻坪A型花岗质岩浆。

目前普遍认为Columbia超大陆是由2.1~1.8Ga全球性碰撞造山带拼合了各相关的克拉通板块而成的,最终的拼合时间为~1.8Ga(Wilde *et al.*, 2002; Zhao *et al.*, 2002, 2009),其裂解发生在大约1.6Ga或者稍微早一点,而所有克拉通板块中均发育的1.35~1.21Ga基性岩墙群记录了其裂解的最终时间(Zhao *et al.*, 2002, 2009; Hou *et al.*, 2008)。华北克拉通的拼合与古元古代末期的"吕梁运动"有关(赵宗溥, 1993; 白瑾等, 1993),区域结晶基底变质年代学资料表明其时代上不晚于1.8Ga(Zhai and Liu, 2003; Zhai and Santosh, 2011; Zhai *et al.*, 2011; 翟明国等, 2014),表明华北克拉通可能为Columbia超大陆的一个组成部分。华北克拉通1.68~1.21Ga发生裂解的岩浆活动产物也较为明显

(*Rämö et al.*, 1995; 杨进辉等, 2005; 任康绪等, 2006; 高维等, 2008; 包志伟等, 2009; Zhang *et al.*, 2007, 2012; Jiang *et al.*, 2011; 李怀坤等, 2011; Wang *et al.*, 2012, 2013; Peng *et al.*, 2013)。麻坪A型花岗岩形成于1600Ma, 与Columbia超大陆开始发生裂解的时间一致,可能代表Columbia超大陆在华北克拉通开始裂解的时间。同时, 1600Ma A型花岗岩与同期的基性岩墙群、双峰式火山岩和碱性岩组合一起较好地指示陆壳减薄和破裂的地质事件(Lu *et al.*, 2002; 陆松年等, 2003),并为Columbia超大陆的裂解提供新的证据(翟明国和彭澎, 2007; Zhao and Zhou, 2009)。

6 结论

(1)华北克拉通南缘麻坪岩体花岗斑岩为过铝质A型花岗岩。

(2)麻坪岩体的形成时代为1600Ma。

(3)麻坪花岗斑岩的岩石地球化学特征和锆石Hf同位素组成表明它们来自太华群高温条件下部分熔融,且与基性岩浆底侵作用有关。

(4)麻坪岩体形成于板内裂谷环境,其形成可能与Columbia超大陆的裂解有关。

致谢 野外工作过程中得到了中国科学院地质与地球物理研究所周艳艳博士、中国科学院广州地球化学研究所孙乾迎硕士的帮助;审稿人张成立教授、赵新福教授提出许多宝贵意见。在此对他们表示衷心感谢!

References

Bai J, Huang GX, Dai FY and Wu CH. 1993. The Precambrian Crustal Evolution of China. Beijing: Geological Publishing House, 199 – 203 (in Chinese)

Bao ZW, Wang Q, Zi F, Tang GJ, Du FJ and Bai GD. 2009. Geochemistry of the Paleoproterozoic Longwangzhuang A-type granites on the southern margin of the North China Craton: Petrogenesis and tectonic implications. Geochimica, 38(6): 509 – 522 (in Chinese with English abstract)

Belousova EA, Griffin WL, O'Reilly SY and Fisher NI. 2002. Igneous zircon: Trace element composition as an indicator of source rock type. Contributions to Mineralogy and Petrology, 143(5): 602 – 622

Blichert-Toft J and Albarède F. 1997. The Lu-Hf isotope geochemistry of chondrites and the evolution of the mantle-crust system. Earth Planet. Sci. Lett., 148(1 – 2): 243 – 258

Bonin B. 2004. Do coeval mafic and felsic magmas in post-collisional to within-plate regimes necessarily imply two contrasting, mantle and crustal, sources? A review. Lithos, 78(1 – 2): 1 – 24

Bonin B. 2007. A-type granites and related rocks: Evolution of a concept, problems and prospects. Lithos, 97(1 – 2): 1 – 29

Cai KD, Sun M, Yuan C, Zhao GC, Xiao WJ, Long XP and Wu FY. 2011. Geochronology, petrogenesis and tectonic significance of peraluminous granites from the Chinese Altai, NW China. Lithos, 127(1 – 2): 261 – 281

Chen YX, Song SG, Niu YL and Wei CJ. 2014. Melting of continental crust during subduction initiation: A case study from the Chaidanuo peraluminous granite in the North Qilian suture zone. Geochimica et Cosmochimica Acta, 132: 311 – 336

Collins WJ, Beams SD, White AJR and Chappell BW. 1982. Nature and origin of A-type granites with particular reference to southeastern Australia. Contrib. Mineral. Petrol., 80(2): 189 – 200

Creaser RA, Price RC and Wormald RJ. 1991. A-type granites revisited: Assessment of a residual-source model. Geology, 19(2): 163 – 166

Diwu CR, Sun Y, Lin CL, Liu XM and Wang HL. 2007. Zircon U-Pb ages and Hf isotopes and their geological significance of Yiyang TTG gneisses from Henan Province, China. Acta Petrologica Sinica, 23(2): 253 – 262 (in Chinese with English abstract)

Diwu CR, Sun Y, Lin CL and Wang HL. 2010. LA-(MC)-ICPMS U-Pb zircon geochronology and Lu-Hf isotope compositions of the Taihua Complex on the southern margin of the North China Craton. Chinese Sci. Bull., 55(23): 2557 – 2571

Diwu CR, Sun Y, Zhao Y and Lai SC. 2014. Early Paleoproterozoic (2.45 ~ 2.20Ga) magmatic activity during the period of global magmatic shutdown: Implications for the crustal evolution of the southern North China Craton. Precambrian Research, 255: 627 – 640

Eby GN. 1992. Chemical subdivision of the A-type granitoids: Petrogenetic and tectonic implications. Geology, 20(7): 641 – 644

Frost CD and Frost BR. 1997. Reduced rapakivi-type granites: The tholeiite connection. Geology, 25(7): 647 – 650

Frost CD, Ramo OT and Dall'Agnol R. 2007. IGCP project 510: A-type granites and related rocks through time. Lithos, 97(1 – 2): Vii – Xiii

Frost CD and Frost BR. 2011. On ferroan (A-type) granitoids: Their compositional variability and modes of origin. Journal of Petrology, 52(1): 39 – 53

Gao SL, Lin JY and Lu YJ. 2013. Formation epoch and its geological implications of Paleoproterozoic A-type granite in Shizuizi of Jingyuan County, Ningxia Province. Acta Petrologica Sinica, 29(8): 2676 – 2684 (in Chinese with English abstract)

Gao W, Zhang CH, Gao LZ, Shi XY, Liu YM and Song B. 2008. Zircon SHRIMP U-Pb age of rapakivi granite in Miyun, Beijing, China, and its tectono-stratigraphic implications. Geological Bulletin of China, 27(6): 793 – 798 (in Chinese with English abstract)

Griffin WL, Pearson NJ, Belousova E, Jackson SE, O'Reilly SY, Van Achterberg E and Shee SR. 2000. The Hf isotope composition of cratonic mantle: LAM-MC-ICPMS analysis of zircon megacrysts in kimberlites. Geochim. Cosmochim. Acta, 64(1): 133 – 147

Haapala I and Rämö OT. 1992. Tectonic setting and origin of the Proterozoic rapakivi granites of the southeastern Fennoscandia. Trans. Roy. Soc. Edinburgh. Earth Sci., 83(1 – 2): 165 – 171

Hou GT, Santosh M, Qian XL, Lister GS and Li JH. 2008. Configuration of the Late Paleoproterozoic supercontinent Columbia: Insights from radiating mafic dyke swarms. Gondwana Research, 14(3): 395 – 409

Hu GH, Hu JL, Chen W and Zhao TP. 2010. Geochemistry and tectonic setting of the 1.78Ga mafic dykes in the Mt. Zhongtiao and Mt. Song areas, the southern margin of the North China Craton. Acta Petrologica Sinica, 26(5): 1563 – 1576 (in Chinese with English abstract)

Hu GH, Zhao TP and Zhou YY. 2014. Depositional age, provenance and tectonic setting of the Proterozoic Ruyang Group, southern margin of the North China Craton. Precambrian Research, 246: 296 – 318

Huang HQ, Li XH, Li WX and Li ZX. 2011. Formation of high $\delta^{18}O$ fayalite-bearing A-type granite by high-temperature melting of granulitic metasedimentary rocks, southern China. Geology, 39(10): 903 – 906

Huang XL, Niu YL, Xu YG, Yang QJ and Zhong JW. 2010. Geochemistry of TTG and TTG-like gneisses from Lushan-Taihua complex in the southern North China Craton: Implications for Late Archean crustal accretion. Precambrian Research, 182(1 – 2): 43 – 56

Huang XL, Wilde SA, Yang QJ and Zhong JW. 2012. Geochronology

and petrogenesis of gray gneisses from the Taihua Complex at Xiong'er in the southern segment of the Trans-North China Orogen: Implications for tectonic transformation in the Early Paleoproterozoic. Lithos, 134 – 135: 236 – 252

Huang XL, Wilde SA and Zhong JW. 2013. Episodic crustal growth in the southern segment of the Trans-North China Orogen across the Archean-Proterozoic boundary. Precambrian Research, 233: 337 – 357

Jiang N, Guo JH and Zhai MG. 2011. Nature and origin of the Wenquan granite: Implications for the provenance of Proterozoic A-type granites in the North China craton. Journal of Asian Earth Sciences, 42(1 – 2): 76 – 82

Kerr A and Fryer BJ. 1993. Nd isotopic evidence for crust-mantle interaction in the generation of A-type granitoid suites in Labrador, Canada. Chem. Geol., 104: 39 – 60

King PL, White AJR, Chappell BW and Allen CM. 1997. Characterization and origin of aluminous A-type granites from the Lachlan Fold Belt, southeastern Australia. J. Petrol., 38(3): 371 – 391

King PL, Chappell BW, Allen CM and White AJR. 2001. Are A-type granites the high-temperature felsic granites? Evidence from fractionated granites of the Wangrah Suite. Australian Journal of Earth Sciences, 48(4): 501 – 514

Li HK, Li HM and Lu SN. 1995. Grain zircon U-Pb ages for volcanic rocks from Tuanshanzi Formation of Changcheng system and their geological implications. Geochimica, 24(1): 43 – 48 (in Chinese with English abstract)

Li HK, Su WB, Zhou HY, Geng JZ, Xiang ZQ, Cui YR, Liu WC and Lu SN. 2011. The base age of the Changchengian System at the northern North China Craton should be younger than 1670Ma: Constraints from zircon U-Pb LA-MC-ICPMS dating of a granite-porphyry dike in Miyun County, Beijing. Earth Science Frontiers, 18(3): 108 – 120 (in Chinese with English abstract)

Liu DY, Wilde SA, Wan YS, Wang SY, Valley JW, Kita N, Dong CY, Xie HQ, Yang CX, Zhang YX and Gao LZ. 2009. Combined U-Pb, hafnium and oxygen isotope analysis of zircons from meta-igneous rocks in the southern North China Craton reveal multiple events in the Late Mesoarchean-Early Neoarchean. Chemical Geology, 261(1 – 2): 140 – 154

Liu XY. 2011. Chronological, petrological and geochemical characteristics of the Paleo-Mesoproterozoic alkali-rich intrusive rocks along the southern part of the North China Craton. Master Degree Thesis. Beijing: Chinese Academy of Geological Sciences (in Chinese with English summary)

Liu Y, Liu HC and Li XH. 1996. Simultaneous and precise determination of 40 trace elements in rock samples using ICP-MS. Geochimica, 25(6): 552 – 558 (in Chinese with English abstract)

Loiselle MC and Wones DR. 1979. Characteristics and origin of anorogenic granites. Geological Society of America Abstracts with Programs, 11(7): 468

Long XP, Sun M, Yuan C, Kröner A and Hu AQ. 2012. Zircon REE patterns and geochemical characteristics of Paleoproterozoic anatectic granite in the northern Tarim Craton, NW China: Implications for the reconstruction of the Columbia supercontinent. Precambrian Research, 222 – 223: 474 – 487

Lu SN, Yang CL, Li HK and Li HM. 2002. A group of rifting events in the terminal Paleoproterozoic in the North China Craton. Gondwana Research, 5(1): 123 – 131

Lu SN, Li HK, Li HM, Song B, Wang SY, Zhou HY and Chen ZH. 2003. U-Pb isotopic ages and their significance of alkaline granite in the southern margin of the North China Craton. Geological Bulletin of China, 22(10): 762 – 768 (in Chinese with English abstract)

Lu SN, Zhao GC, Wang HC and Hao GJ. 2008. Precambrian metamorphic basement and sedimentary cover of the North China Craton: A review. Precambrian Research, 160(1 – 2): 77 – 93

Maniar PD and Piccoli PM. 1989. Tectonic discrimination of granitoids. Geological Society of America Bulletin, 101: 635 – 643

Martínez EM, Villaseca C, Orejana D, Pérez-Soba C, Belousova E and Andersen T. 2014. Tracing magma sources of three different S-type peraluminous granitoid series by in situ U-Pb geochronology and Hf isotope zircon composition: The Variscan Montes de Toledo batholith (central Spain). Lithos, 200 – 201: 273 – 298

Miller CF, McDowell SM and Mapes RW. 2003. Hot and cold granites? Implications of zircon saturation temperatures and preservation of inheritance. Geology, 31(6): 529 – 532

Mingram B, Trumbull RB, Littman S and Gerstenberger H. 2000. A petrogenetic study of anorogenic felsic magmatism in the Cretaceous Paresis ring complex, Namibia: Evidence for mixing of crust and mantle-derived components. Lithos, 54(1 – 2): 1 – 22

Montel JM and Vielzeuf D. 1997. Partial melting of metagreywackes, Part Ⅱ. Compositions of minerals and melts. Contributions to Mineralogy and Petrology, 128(2 – 3): 176 – 196

Mushkin A, Navon O, Halicz L, Hartmann G and Stein M. 2003. The petrogenesis of A-type magmas from the Amram Massif, southern Israel. J. Petrol., 44(5): 815 – 832

Patiño Douce AE and Harris N. 1998. Experimental constraints on Himalayan anatexis. Journal of Petrology, 39(4): 689 – 710

Pearce JA, Harris NBW and Tindle AG. 1984. Trace-element discrimination diagrams for the tectonic interpretation of granitic-rocks. Journal of Petrology, 25(4): 956 – 983

Pearce JA. 1996. Sources and settings of granitic rocks. Episodes, 19(4): 120 – 125

Peng P, Zhai MG, Zhang HF, Zhao TP and Ni ZY. 2004. Geochemistry and geological significance of the 1.8Ga mafic dyke swarms in the North China Craton: An example from the juncture of Shanxi, Hebei and Inner Mongolia. Acta Petrologica Sinica, 20(3): 439 – 456 (in Chinese with English abstract)

Peng P, Zhai MG, Zhang HF and Guo JH. 2005. Geochronological constraints on the Paleoproterozoic evolution of the North China craton: SHRIMP zircon ages of different types of mafic dikes. International Geology Review, 47(5): 492 – 508

Peng P, Liu F, Zhai MG and Guo JH. 2012. Age of the Miyun dyke swarm: Constraints on the maximum depositional age of the Changcheng System. Chinese Sci. Bull., 57(1): 105 – 110

Peng TP, Wilde SA, Fan WM, Peng BX and Mao YS. 2013. Mesoproterozoic high Fe-Ti mafic magmatism in western Shandong, North China Craton: Petrogenesis and implications for the final breakup of the Columbia supercontinent. Precambrian Research, 235: 190 – 207

Rämö OT, Haapala I, Vaasjoki M, Yu JH and Fu HQ. 1995. 1700Ma Shachang complex, Northeast China: Proterozoic rapakivi granite not associated with Paleoproterozoic orogenic crust. Geology, 23(9): 815 – 818

Ren KX, Yan GH, Cai JH, Mu BL, Li FT, Wang YB and Chu ZY. 2006. Chronology and geological implication of the Paleo-Mesoproterozoic alkaline-rich intrusions belt from the northern part in the North China Craton. Acta Petrologica Sinica, 22(2): 377 – 386 (in Chinese with English abstract)

Shi Y, Yu JH, Xu XS, Tang HF, Qiu JS and Chen LH. 2011. U-Pb ages and Hf isotope compositions of zircons of Taihua Group in Xiaoqinling area, Shaanxi Province. Acta Petrologica Sinica, 27(10): 3095 – 3108 (in Chinese with English abstract)

Söderlund U, Patchett PJ, Vervoort JD and Lsachsen CE. 2004. The ^{176}Lu decay constant determined by Lu-Hf and U-Pb isotope systematics of Precambrian mafic intrusions. Earth Planet. Sci. Lett., 219(3 – 4): 311 – 324

Sun SS and McDonough WF. 1989. Chemical and isotopic systematic of oceanic basalts: Implications for mantle composition and process. In: Saunders AD and Norry MJ (eds.). Magmatism in the Ocean Basins. Geological Society, London, Special Publication, 42(1): 313 – 345

Sylvester PJ. 1998. Post-collisional strongly peraluminous granites. Lithos, 45(1 – 4): 29 – 44

Vervoort JD, Patchett PJ, Gehrels GE and Nutman AP. 1996. Constraints on early Earth differentiation from hafnium and neodymium isotopes. Nature, 379(6566): 624 – 627

Wang XL, Jiang SY, Dai BZ and Kern J. 2012. Lithospheric thinning and reworking of Late Archean juvenile crust on the southern margin of the North China Craton: Evidence from the Longwangzhuang Paleoproterozoic A-type granites and their surrounding Cretaceous adakite-like granites. Geological Journal, 48(5): 498 – 515

Wang YJ, Fan WM, Zhang YH, Guo F, Zhang HF and Peng TP. 2004. Geochemical, $^{40}Ar/^{39}Ar$ geochronological and Sr-Nd isotopic constraints on the origin of Paleoproterozoic mafic dikes from the southern Taihang Mountains and implications for the ca. 1800Ma event of the North China Craton. Precambrian Research, 135(1 – 2): 55 – 77

Wang YJ, Zhao GC, Cawood PA, Fan WM, Peng TP and Sun LH. 2008. Geochemistry of Paleoproterozoic (1770Ma) mafic dikes from the Trans-North China Orogen and tectonic implications. Journal of Asian Earth Sciences, 33(1 – 2): 61 – 77

Wang W, Liu SW, Bai X, Li QG, Yang PT, Zhao Y, Zhang SH and Guo RR. 2013. Geochemistry and zircon U-Pb-Hf isotopes of the Late Paleoproterozoic Jianping diorite-monzonite-syenite suite of the North China Craton: Implications for petrogenesis and geodynamic setting. Lithos, 162 – 163: 175 – 194

Watson EB and Harrison TM. 1983. Zircon saturation revisited: Temperature and composition effects in a variety of crustal magma type. Earth Planet. Sci. Lett., 64(2): 295 – 304

Whalen JB, Currie KL and Chappell BW. 1987. A-type granites: Geochemical characteristics, discrimination and petrogenesis. Contrib. Miner. Petrol., 95(4): 407 – 419

Wilde SA, Zhao GC and Sun M. 2002. Development of the North China Craton during the Late Archaean and its final amalgamation at 1.8Ga: Some speculations on its position within a global Palaeoproterozoic supercontinent. Gondwana Research, 5(1): 85 – 94

Wilson M. 1989. Igneous Petrogenesis: A Global Tectonic Approach. Chapman & Hall, London, 13 – 34

Wu FY, Sun DY, Li H, Jahn BM and Wilde S. 2002. A-type granites in northeastern China: Age and geochemical constraints on their petrogenesis. Chemical Geology, 187(1 – 2): 143 – 173

Wu FY, Yang YH, Xie LW, Yang JH and Xu P. 2006. Hf isotopic compositions of the standard zircons and baddeleyites used in U-Pb geochronology. Chemical Geology, 234(1 – 2): 105 – 126

Wu YB and Zheng YF. 2004. Genesis of zircon and its constraints on the interpretation of U-Pb age. Chinese Science Bulletin, 49(15): 1554 – 1569

Xu XS, Griffin WL, Ma X, O'Reilly SY, He ZY and Zhang CL. 2009. The Taihua group on the southern margin of the North China craton: Further insights from U-Pb ages and Hf isotope compositions of zircons. Mineralogy and Petrology, 97(1 – 2): 43 – 59

Yan J, Peng G, Liu JM, Li QZ, Chen ZH, Shi L, Liu XQ and Jiang ZZ. 2012. Petrogenesis of granites from Fanchang district, the Lower Yangtze: Zircon geochronology and Hf-O isotopes constrains. Acta Petrologica Sinica, 28(10): 3209 – 3227 (in Chinese with English abstract)

Yang CX, Wang SY, Liu ZH, Lei ZH and Yang CQ. 2008. Mesoarchean-Neoarchean grey gneiss in the Lushan area, Henan Province. Geological Review, 54(3): 327 – 334 (in Chinese with English abstract)

Yang JH, Wu FY, Liu XM and Xie LW. 2005. Zircon U-Pb ages and Hf isotopes and their geological significance of the Miyun rapakivi granites from Beijing, China. Acta Petrologica Sinica, 21(6): 1633 – 1644 (in Chinese with English abstract)

Yang JH, Wu FY, Chung SL, Wilde SA and Chu MF. 2006. A hybrid origin for the Qianshan A-type granite, Northeast China: Geochemical and Sr-Nd-Hf isotopic evidence. Lithos, 89(1 – 2): 89 – 106

Zhai MG and Liu WJ. 2003. Palaeoproterozoic tectonic history of the North China craton: A review. Precambrian Research, 122(1 – 4): 183 – 199

Zhai MG and Peng P. 2007. Paleoproterozoic event in the North China Craton. Acta Petrologica Sinica, 23(11): 2665 – 2682 (in Chinese with English abstract)

Zhai MG and Santosh M. 2011. The Early Precambrian odyssey of the North China Craton: A synoptic overview. Gondwana Research, 20(1): 6 – 25

Zhai MG, Santosh M and Zhang LC. 2011. Precambrian geology and tectonic evolution of the North China Craton. Gondwana Research, 20(1): 1 – 5

Zhai MG, Hu B and Peng P. 2014. Meso-Neoproterozoic magmatic events and multi-stage rifting in the NCC. Earth Science Frontiers, 21(1): 100 – 119 (in Chinese with English abstract)

Zhang J, Zhang HF and Lu XX. 2013. Zircon U-Pb age and Lu-Hf isotope constraints on Precambrian evolution of continental crust in the Songshan area, the south-central North China Craton. Precambrian Research, 226: 1 – 20

Zhang SH, Liu SW, Zhao Y, Yang JH, Song B and Liu XM. 2007. The 1.75 ~ 1.68Ga anorthosite-mangerite-alkali granitoid-rapakivi granite suite from the northern North China Craton: Magmatism related to a Paleoproterozoic orogen. Precambrian Research, 155(3 – 4): 287 – 312

Zhang SH, Zhao Y and Santosh M. 2012. Mid-Mesoproterozoic bimodal magmatic rocks in the northern North China Craton: Implications for magmatism related to breakup of the Columbia supercontinent. Precambrian Research, 222 – 223: 339 – 367

Zhao GC, Cawood PA, Wilde SA and Sun M. 2002. Review of global 2.1 ~ 1.8Ga orogens: Implications for a pre-Rodinia supercontinent. Earth-Science Reviews, 59(1 – 4): 125 – 162

Zhao GC, He YH and Sun M. 2009. The Xiong'er volcanic belt at the southern margin of the North China Craton: Petrographic and geochemical evidence for its outboard position in the Paleo-Mesoproterozoic Columbia Supercontinent. Gondwana Research, 16(2): 170 – 181

Zhao TP, Zhou MF, Zhai MG and Xia B. 2002. Paleoproterozoic rift-related volcanism of the Xiong'er Group, North China Craton: Implications for the breakup of Columbia. International Geology Review, 44(4): 336 – 351

Zhao TP, Chen FK, Zhai MG and Xia B. 2004. Single zircon U-Pb ages and their geological significance of the Damiao anorthosite complex, Hebei Province, China. Acta Petrologica Sinica, 20(3): 685 – 690 (in Chinese with English abstract)

Zhao TP and Zhou MF. 2009. Geochemical constraints on the tectonic setting of Paleoproterozoic A-type granites in the southern margin of the North China Craton. Journal of Asian Earth Sciences, 36(2 – 3): 183 – 195

Zhao XF, Zhou MF, Li JW and Wu FY. 2008. Association of Neoproterozoic A- and I-type granites in South China: Implications for generation of A-type granites in a subduction-related environment. Chemical Geology, 257(1 – 2): 1 – 15

Zhao ZP. 1993. Precambrian Crustal Evolution of the Sino-Korean Paraplatform. Beijing: Science Press (in Chinese)

Zhou YY, Zhai MG, Zhao TP, Lan ZW and Sun QY. 2014. Geochronological and geochemical constraints on the petrogenesis of the Early Paleoproterozoic potassic granite in the Lushan area, southern margin of the North China Craton. Journal of Asian Earth Sciences, 94: 190 – 204

附中文参考文献

白瑾, 黄学光, 戴风岩, 吴昌华. 1993. 中国前寒武纪地壳演化. 北京: 地质出版社, 199 – 203

包志伟, 王强, 资锋, 唐功建, 杜凤军, 白国典. 2009. 龙王碴 A 型花岗岩地球化学特征及其地球动力学意义. 地球化学, 38(6): 509 – 522

第五春荣, 孙勇, 林慈銮, 柳小明, 王洪亮. 2007. 豫西宜阳地区 TTG 质片麻岩锆石 U-Pb 定年和 Hf 同位素地质学. 岩石学报, 23(2): 253 – 262

第五春荣，孙勇，林慈銮，王洪亮. 2010. 河南鲁山地区太华杂岩LA-(MC)-ICPMS锆石U-Pb年代学及Hf同位素组成. 科学通报，55(21)：2112－2123

高山林，林晋炎，陆彦俊. 2013. 宁夏泾源石咀子古元古代A型花岗岩的形成时代及其地质意义. 岩石学报，29(8)：2676－2684

高维，张传恒，高林志，史晓颖，刘耀明，宋彪. 2008. 北京密云环斑花岗岩的锆石SHRIMP U-Pb年龄及其构造意义. 地质通报，27(6)：793－798

胡国辉，胡俊良，陈伟，赵太平. 2010. 华北克拉通南缘中条山-嵩山地区1.78Ga基性岩墙群的地球化学特征及构造环境. 岩石学报，26(5)：1563－1576

李怀坤，李惠民，陆松年. 1995. 长城系团山子组火山岩颗粒锆石U-Pb年龄及其地质意义. 地球化学，24(1)：43－48

李怀坤，苏文博，周红英，耿建珍，相振群，崔玉荣，刘文灿，陆松年. 2011. 华北克拉通北部长城系底界年龄小于1670Ma：来自北京密云花岗斑岩岩脉锆石LA-MC-ICPMS U-Pb年龄的约束. 地学前缘，18(3)：108－120

柳晓艳. 2011. 华北克拉通南缘古-中元古代碱性岩岩石地球化学与年代学研究及其地质意义. 硕士学位论文. 北京：中国地质科学院

刘颖，刘海臣，李献华. 1996. 用ICP-MS准确测定岩石样品中40余种微量元素. 地球化学，25(6)：552－558

陆松年，李怀坤，李惠民，宋彪，王世炎，周红英，陈志宏. 2003. 华北克拉通南缘龙王碾碱性花岗岩U-Pb年龄及其地质意义. 地质通报，22(10)：762－768

彭澎，翟明国，张华峰，赵太平，倪志耀. 2004. 华北克拉通1.8Ga镁铁质岩墙群的地球化学特征及其地质意义：以晋冀蒙交界地区为例. 岩石学报，20(3)：439－456

彭澎，刘富，翟明国，郭敬辉. 2011. 密云岩墙群的时代及其对长城系底界年龄的制约. 科学通报，56(35)：2975－2980

任康绪，阎国翰，蔡剑辉，牟保磊，李凤棠，王彦斌，储著银. 2006. 华北克拉通北部地区古-中元古代富碱侵入岩年代学及意义. 岩石学报，22(2)：377－386

时毓，于津海，徐夕生，唐红峰，邱检生，陈立辉. 2011. 陕西小秦岭地区太华群的锆石U-Pb年龄和Hf同位素组成. 岩石学报，27(10)：3095－3108

闫峻，彭戈，刘建敏，李全忠，陈志洪，史磊，刘晓强，姜子朝. 2012. 下扬子繁昌地区花岗岩成因：锆石年代学和Hf-O同位素制约. 岩石学报，28(10)：3209－3227

杨长秀，王世炎，刘振宏，雷正化，杨长青. 2008. 河南鲁山地区中-新太古代灰色片麻岩. 地质论评，54(3)：327－334

杨进辉，吴福元，柳小明，谢烈文. 2005. 北京密云环斑花岗岩锆石U-Pb年龄和Hf同位素及其地质意义. 岩石学报，21(6)：1633－1644

翟明国，彭澎. 2007. 华北克拉通古元古代构造事件. 岩石学报，23(11)：2665－2682

翟明国，胡波，彭澎，赵太平. 2014. 华北中-新元古代的岩浆作用与多期裂谷事件. 地学前缘，21(1)：100－119

赵太平，陈福坤，翟明国，夏斌. 2004. 河北大庙斜长岩杂岩体锆石U-Pb年龄及其地质意义. 岩石学报，20(3)：685－690

赵宗溥. 1993. 中朝准地台前寒武纪地壳演化. 北京：科学出版社